Proceedings of the 12th International Conference on
Aluminium Alloys, September 5-9, 2010, Yokohama, Japan

pp. 363-370

Effect of Experimental Humidity on Fatigue Fracture of 6XXX-series Aluminum Alloys

Koji Ichitani and Katsumi Koyama
Technical Research Div., Furukawa-Sky Aluminum Corp.,
1351, Uwanodai, Fukaya-city, Saitama Prefecture 366-8511, Japan

Fatigue tests under controlled experimental humidity were conducted to reveal the effect of hydrogen on 6XXX-series aluminum alloys. This is because under a humidified air condition hydrogen atoms are generated through a reaction between successively exposed aluminum surface and vapor water, and then the experimental condition of high pressure hydrogen gas environment can be readily simulated. In order to examine intrinsic hydrogen embrittlement behavior of 6XXX-seriese alloys during fatigue fracture, a ternary Al-Mg-Si alloy was subjected to the test. The fatigue life of the alloy was substantially lower under a humidified air condition than an inert dry nitrogen-gas condition. The effect of additive elements such as Cu, Cr and Fe on the fatigue life of the ternary alloy was examined, and it was revealed that the fatigue life of a Cu-containing alloy was not decreased under humidified air condition. This result suggests that Cu has an effect of decreasing hydrogen embrittlement sensitivity of 6XXX-series alloys.

Keywords: *Hydrogen embrittlement, Fatigue fracture, 6XXX-series alloy, Intergranular cracking.*

1. Introduction

A fuel-cell-powered car has been developed in the world to reduce the emission of green house gases. Aluminum alloys have been applied to the liner of high pressure hydrogen-gas tanks loaded on the car because of their superior lightweight properties and airtightness. Currently in Japan, the safety of an AA6061 alloy under high pressure hydrogen-gas has been confirmed and has already been applied to the liner. In the near future, the usage of 6XXX-series alloys of higher strength is expected. For the purpose of assuring the long-term safety of a higher strength alloy, it is important to understand the hydrogen embrittlement behavior of 6XXX-series alloys intrinsically. In particular, the effect of hydrogen on their fatigue property is important, because the liner of the tank undergoes repetitive stress in response to charge and discharge of hydrogen gas.

In the present study, fatigue tests under controlled experimental humidity were conducted to reveal the effect of hydrogen. This is because under a humidified air condition hydrogen atoms are generated through a reaction between successively exposed aluminum surface and vapor water, and then the experimental condition of a high pressure hydrogen gas environment can be readily simulated [1]. In order to examine the intrinsic hydrogen embrittlement behavior of 6XXX-seriese alloys during the process of fatigue fracture, a ternary Al-Mg-Si alloy was subjected to the test with a comparison AA6061 alloy of the same Mg and Si compositions. Additionally, the effects of addition of elements such as Cu, Cr and Fe to the Al-Mg-Si alloy on the hydrogen embrittlement behavior were examined.

2. Experimental Procedure

2.1 Materials

Chemical compositions of aluminum alloys used in the present study are provided in Table 1 in comparison with the composition ranges of the AA6061 alloy. A 6061-Max alloy contains maximum amounts of Mg and Si within the ranges of the AA6061 alloy and other additive elements of normal amounts. Whereas, we tried to make the ternary Al-Mg-Si alloy which contained the almost same amounts of Mg and Si as the 6061-Max alloy, but the alloy substantially contained small amount of inevitable impurity Fe. The Al-Mg-Si-Cu, Al-Mg-Si-Cr and Al-Mg-Si-Fe alloys also contain the almost same amounts of Mg and Si, and additionally they also contain normal amounts of Cu, Cr and Fe respectively with inevitable impurity Fe.

Alloy ingots of these compositions produced by direct-chill casting were homogenized, and then scalped from a thickness of 80 mm to 70 mm. The scalped ingots were hot-rolled to 4 mm thickness and then cold-rolled to 1 mm thickness. The cold rolled alloy sheets were solution-heat-treated at 540˚C for 48 h, and then quenched into water. After that, they were subjected to natural aging of 48 h followed by artificial aging at 175˚C for 8 h.

The heat-treated sheets were subjected to metallographic observation by an optical microscope, after polished and electrolytically etched in Barker's regent under a voltage of 30 V for 2 min. In addition, tensile specimens were machined from the alloy sheets with the tensile axis across the sheet rolling direction, and subjected to tensile tests with a cross head speed of 5 mm/min to measure their mechanical properties, tensile strength (TS), yield strength (YS) and elongation (EL).

Table 1. Chemical compositions (mass %) of the alloys.

	Si	Fe	Cu	Mn	Mg	Cr	Al
6061-Max	0.83	0.27	0.28	0.06	1.22	0.17	bal
Al-Mg-Si	0.82	0.06	-	-	1.19	-	bal
Al-Mg-Si-Cu	0.78	0.07	0.30	-	1.18	-	bal
Al-Mg-Si-Cr	0.79	0.07	-	-	1.17	0.18	bal
Al-Mg-Si-Fe	0.81	0.31	-	-	1.21	-	bal
AA6061	0.40-0.8	<0.7	0.15-0.40	<0.15	0.8-1.2	0.04-0.35	

2.2 Fatigue tests under controlled humidity

For the fatigue tests, a servohyraulic Shimadzu machine was used. Axial load fatigue test specimens shown in Fig. 1 were machined from the heat-treated alloy sheets with a tensile axis across a sheet rolling direction. The tests were performed for a constant stress ratio, R = 0.1, and a frequency used was 70 Hz. The fatigue tests were conducted under three experimental environments, 90 % relative humidity air (RH90%), RH40% and dry nitrogen gas (DNG). In the former two cases, the specimen mounted on the fatigue test machine was covered up by a constant temperature and humidity chamber, and a constant temperature in the chamber was 20 ℃. On the other hand, the DNG environment was achieved by continual flow of dry nitrogen gas through an acrylic chamber covering the specimen with a flow rate of 1 liter/min. An actual measurement value of relative humidity in the acrylic chamber was 5 - 8 % at experimental temperatures of 20 - 25℃.

The fracture surfaces of the fatigue specimens were observed under a scanning electron microscope (SEM) to examine their fracture patterns.

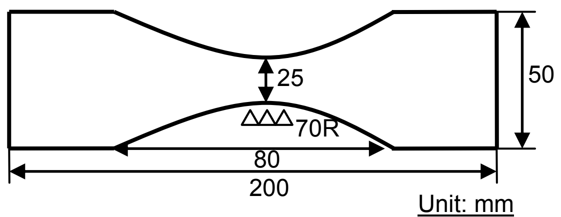

Fig. 1. Axial load fatigue test specimen

3. Results and Discussion

3.1 Microstructure and mechanical properties

Fig. 2 shows microstructure of the heat-treated alloys. It should be noted that the alloys greatly differ in grain size. The 6061-Max alloy exhibits the finest grain structure of the alloys, because this alloy contains both Cr and Fe which contribute to refinement of the grain structure. The grain size of the Al-Mg-Si-Cr alloy is smaller than that of the Al-Mg-Si-Fe alloy, suggesting that the grain refinement effect of Cr is larger than that of Fe in the present fabrication process. The grain sizes of the Al-Mg-Si and the Al-Mg-Si-Cu alloys which are free from these refinement elements are about the same level and larger than those of the other alloys.

The mechanical properties of the alloys are listed in Table 2. The strengths of the 6061-Max and the Al-Mg-Si-Cu alloys both of which contain Cu are higher than those of the other Cu-free alloys. This was because age-hardenabilities of the Al-Mg-Si alloys were increased by the addition of Cu.

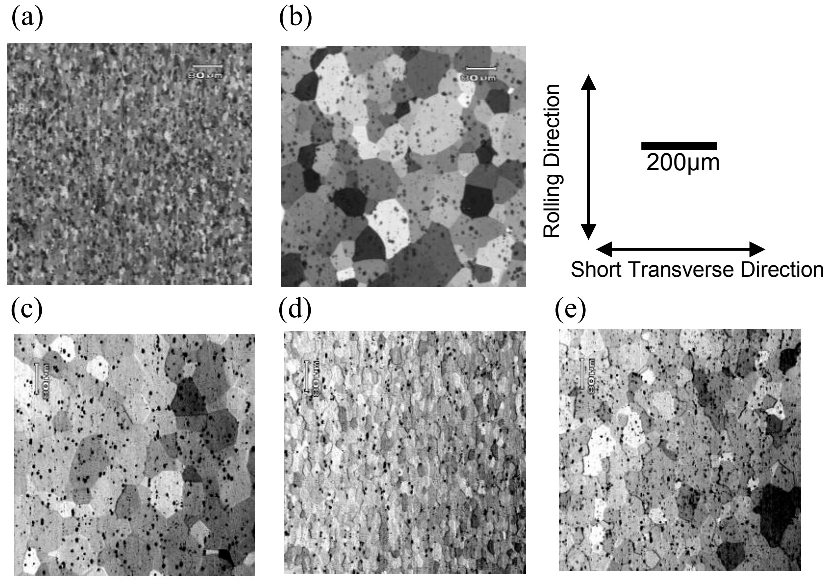

Fig. 2. Optical micrographs of the alloys. (a) 6061-Max, (b) Al-Mg-Si, (c) Al-Mg-Si-Cu, (d) Al-Mg-Si-Cr, (e) Al-Mg-Si-Fe.

Table 2. Mechanical properties of the alloys.

	TS, MPa	YS, MPa	EL, %
6061-Max	343	298	12
Al-Mg-Si	293	259	11
Al-Mg-Si-Cu	337	302	13
Al-Mg-Si-Cr	302	261	16
Al-Mg-Si-Fe	289	242	16

3.2 Fatigue test results 1: comparison between 6061-Max and Al-Mg-Si

Fig. 3 shows S-N curves for the 6061-Max and the Al-Mg-Si alloys. These two alloys exhibit obvious difference in the effect of experimental humidity on their S-N curves. In the case of the 6061-Max alloy, although the cyclic lives under RH90% are somewhat lower than those under other less humidified air conditions, the cyclic lives not always decrease with humidity and the effect of humidity on its cyclic lives are not so significant. On the other hand, the cyclic lives of the Al-Mg-Si alloy drastically decrease with humidity. The cyclic lives for a stress amplitude of 130 MPa under RH40% and RH90% are only from one fifth to one third of those under DNG.

In order to reveal the cause of decrease in the fatigue life of the Al-Mg-Si alloy under the humidified air conditions severer than DNG, the fracture surfaces near their fatigue crack initiation sites formed under the test condition of a stress amplitude of 130 MPa were observed by SEM. Observation results are shown in Fig. 4. Fatigue crack initiation sites estimated from macroscopic fracture patterns are indicated by arrows in this figure. The fracture surface is divided into three regions on the basis of their fractographic characters: (i) an intergranular cracking (IGC) region surrounded by the solid line, (ii) a fatigue crack growth region surrounded by the dotted line and (iii) a final fracture region indicated by the outside of the dotted line. The magnification images of the IGC regions are also shown in the same figure. Many grain boundary surfaces in the IGC regions are free from ductile dimples, suggesting that this IGC is brittle fracture caused by hydrogen embrittlement (HE). The occurrence of IGC in a brittle manner was reported for an excess-Si type 6XXX-series alloy of coarse grain structure studied by a slow strain tensile test [2]. As can be noted from Fig. 4, the area of the IGC region tends to increase with experimental humidity. In Fig. 5, numbers of cycles to failure for Al-Mg-Si under stress amplitude conditions of 120 MPa and 130 MPa are plotted as a function of the IGC areas. This figure shows that cyclic lives decrease with increasing IGC areas near the crack initiation sites for both stress amplitude conditions examined.

From the above results, the decrease in cyclic lives of the Al-Mg-Si alloy with experimental humidity (Fig. 3-(b)) was probably attributed to increase in fatigue crack growth rate in a very earlier stage of crack growth by the occurrence of the brittle IGC near the crack initiation site. Another potential explanation was that the decrease in fatigue lives resulted mainly from increase in crack growth rate in an intermediate stage of fatigue crack growth by HE. To examine this influence, the striation patterns of the Al-Mg-Si alloy were observed. Fig. 6 shows the striation patterns at regions 0.5 mm away from the estimated crack initiation sites. It was difficult to compare the fatigue crack growth rate between under DNG and RH90% conditions from the patterns because the striation interval varied considerably with observation locations. In the present study, we could not distinguish a difference in the striation interval between the two experimental conditions, suggesting that possibility for difference in fatigue crack growth rate in an intermediate crack growth stage was not significant. Whatever the case, in order to reveal the mechanism, further studies on the time-dependent growth of the fatigue crack for the alloy will be necessary.

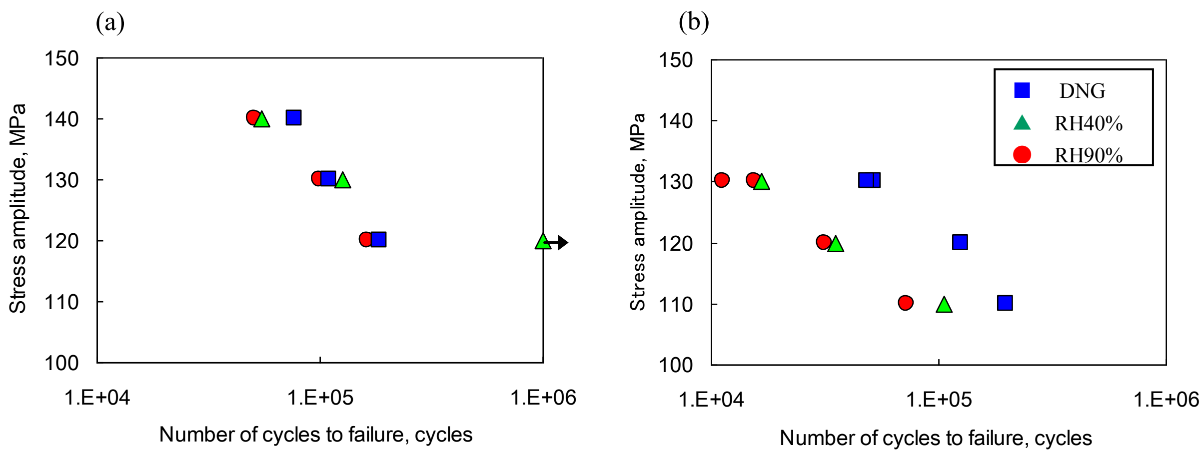

Fig. 3. S-N curves under controlled experimental humidity environments. (a) 6061-Max and (b) Al-Mg-Si.

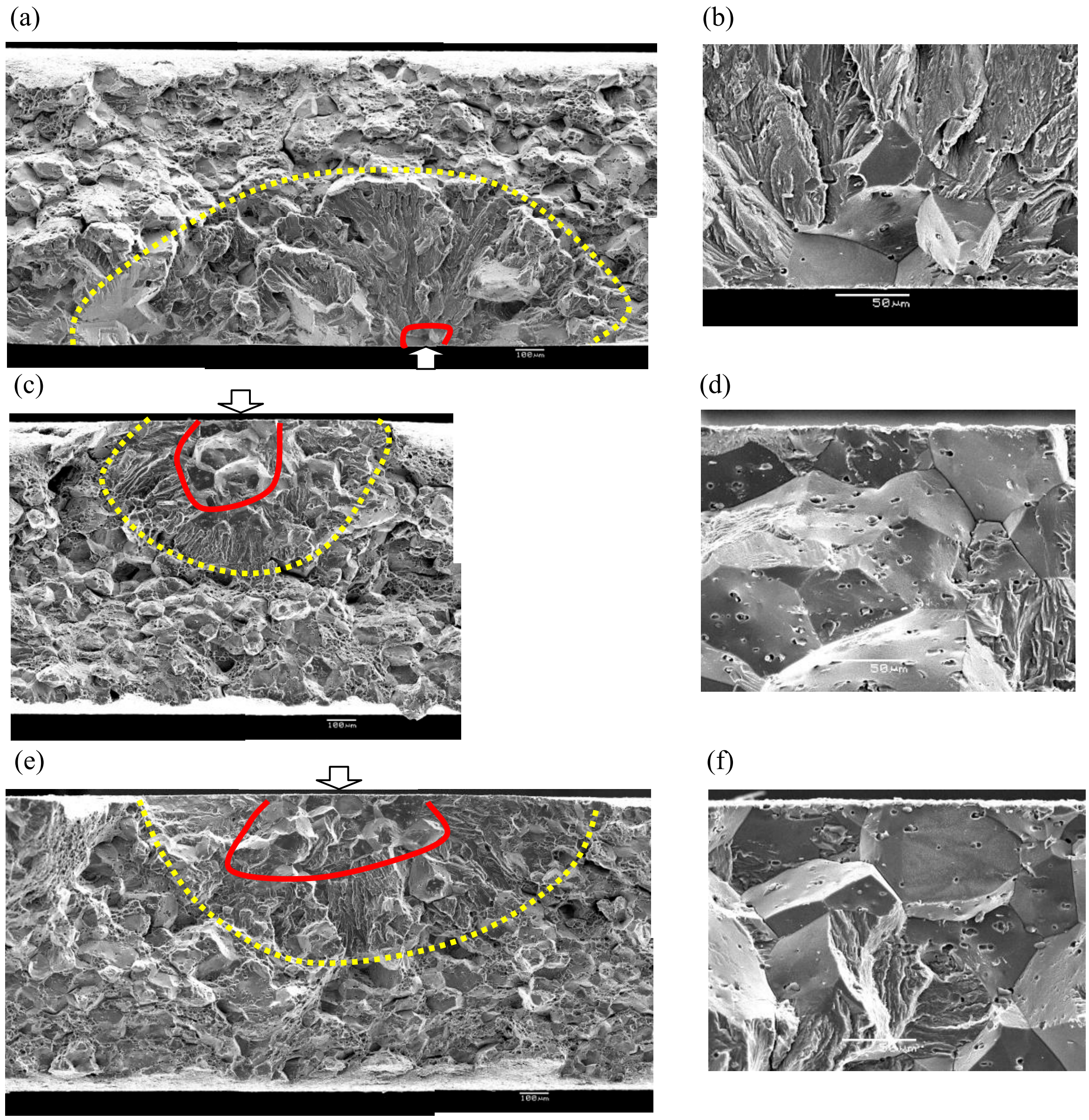

Fig. 4. Fracture surfaces near the fatigue crack initiation sites of the Al-Mg-Si alloy tested at a stress amplitude of 130 MPa: (a) tested under DNG, (c) under RH40%, (e) under RH90%. Magnification image of IGC regions of the fracture surfaces: (b) tested under DNG, (d) under RH40%, (f) under RH90%.

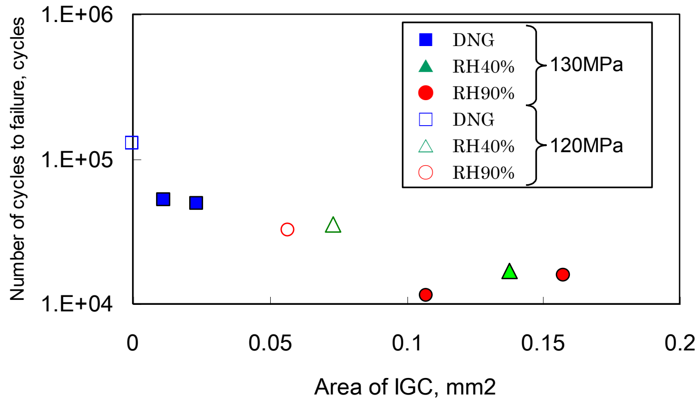

Fig. 5. The numbers of cycles to failure are plotted as a function of areas of IGC regions near the fatigue crack initiation sites.

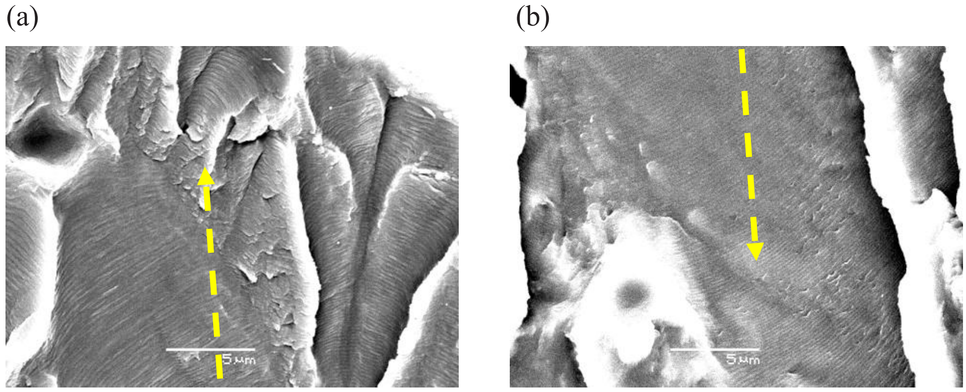

Fig. 6. Striation patterns in the fracture surfaces of the Al-Mg-Si alloy tested at a stress amplitude of 130 MPa under (a) DNG and (b) RH90%. Macroscopic fatigue crack growth directions are indicated by arrows.

3.3 Fatigue test results 2: effect of the additive elements

The Al-Mg-Si-Cu, Al-Mg-Si-Cr and Al-Mg-Si-Fe alloys were subjected to the fatigue test under DNG and RH90% conditions to reveal the effect additive elements on the HE sensitivity of the Al-Mg-Si alloy in the fatigue fracture. Fig. 7 shows S-N curves for these alloys. Among the additive elements, only Cu exhibits a clear effect of decreasing the HE sensitivity of the Al-Mg-Si alloy, and cyclic lives under RH90% are as long as those under DNG (Fig. 7-(a)). On the other hand, in the case of the Al-Mg-Si-Fe alloy, the HE trend of the Al-Mg-Si alloy remains unchanged (Fig. 8-(c)). As for the Al-Mg-Si-Cr alloy, although the HE trend is not so strong, the cyclic lives under RH90% are shorter than those under DNG as a whole (Fig. 8-(b)).

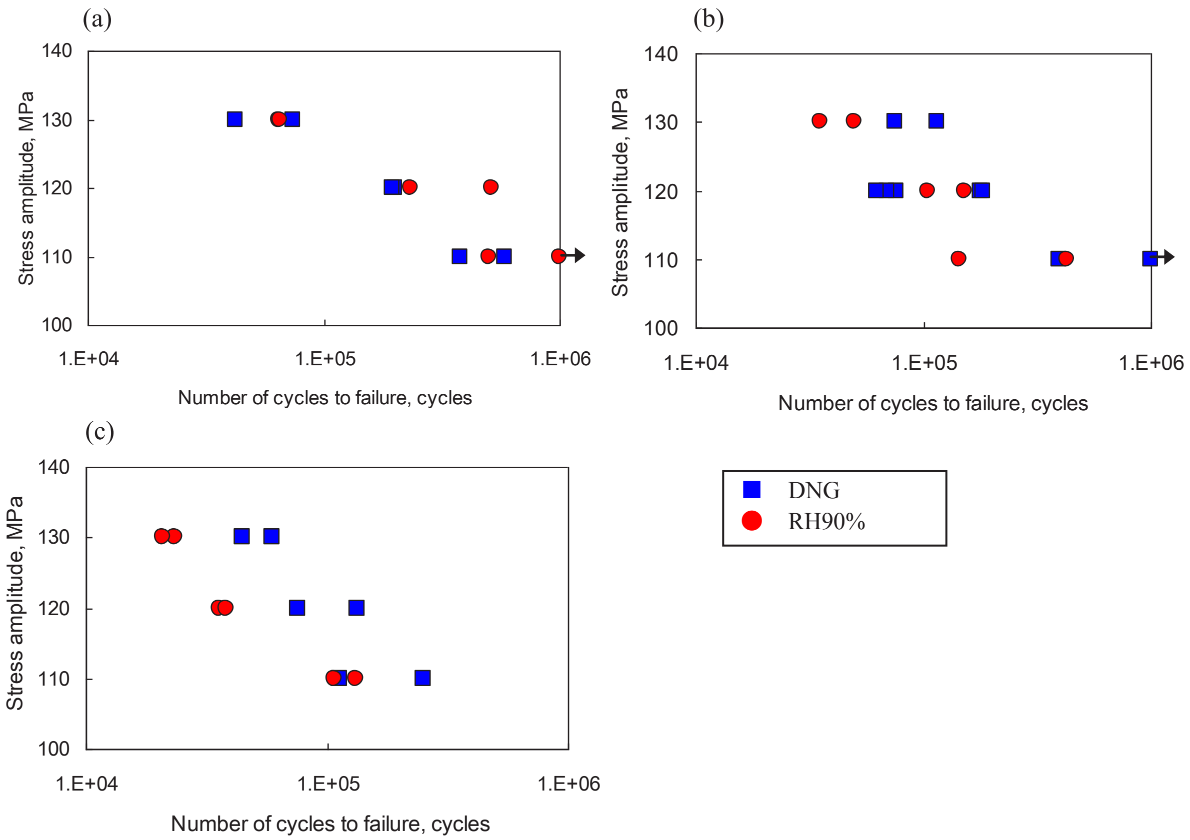

Fig. 7. S-N curves under controlled experimental humidity. (a) Al-Mg-Si-Cu, (b) Al-Mg-Si-Cr and (c) Al-Mg-Si-Fe.

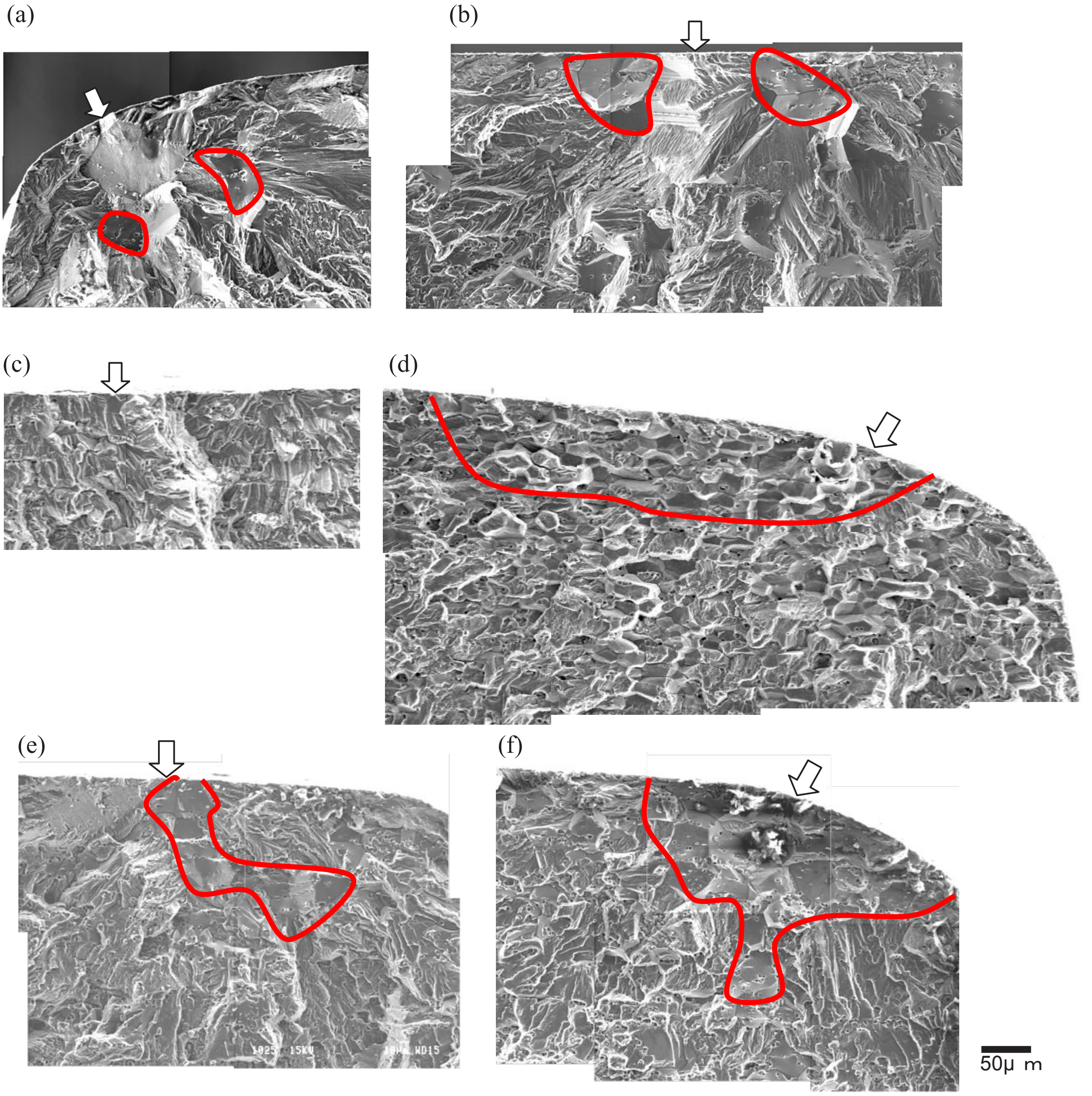

Fig. 8. Fracture surfaces of the alloys under controlled experimental humidity: (a) Al-Mg-Si-Cu, under DNG, (b) Al-Mg-Si-Cu, under RH90%, (c) Al-Mg-Si-Cr, under DNG, (d) Al-Mg-Si-Cr, under RH90%, (e) Al-Mg-Si-Fe, under DNG, (f) Al-Mg-Si-Fe under RH90%.

The fracture surfaces of these alloys tested at a stress amplitude of 130 MPa are shown in Fig. 8. Fatigue crack initiation sites are indicated by the arrows in this figure. Although the Al-Mg-Si-Cu alloy exhibits IGC regions near its crack initiation site both under DNG and RH90% conditions, the IGC area of this alloy under RH90% (Fig. 8-(b)) is much smaller than that observed in the Al-Mg-Si alloy under the same RH90% condition (Fig. 5-(e)). This result suggests that the decrease in HE sensitivity by Cu addition (Fig. 7-(a)) is attributed to the inhibition of IGC near the fatigue crack initiation site. Although the mechanism of the inhibition of IGC by Cu addition was not revealed in the present study, change in hydrogen accumulation sites, such as precipitates in a matrix and grain boundaries, might be deserve considering.

On the other hand, the fracture surfaces of the Al-Mg-Si-Cr alloy suggest the occurrence of a typical HE phenomenon. In the case of DNG, there is no IGC near the fatigue crack initiation site (Fig. 7-(c)). However, under RH90%, an IGC region of a considerably large area extends around the crack initiation site (Fig. 7-(d)). The fact that the Al-Mg-Si-Cr alloy exhibits no IGC under DNG despite the presence of just a little IGC under DNG in the Al-Mg-Si-Cu alloy having lower HE sensitivity may be attributed to difference in grain sizes between the two alloys as shown in Fig. 2. Resistance to the occurrence of IGC increases with grain size independently of HE sensitivity, and thus the Al-Mg-Si-Cr alloy which has a finer grain structure is interrupted to have exhibited no IGC under the milder DNG condition. Whereas, the fracture surfaces of the Al-Mg-Si-Fe alloy present IGC regions near their crack initiation sites under both DNG and RH90% conditions, and an IGC area under RH90% is lager than that under DNG.The same trends were recognized for the ternary Al-Mg-Si alloy (Fig. 4). This result can be attributed to the following common features between the Al-Mg-Si and the Al-Mg-Si-Fe alloys: high HE sensitivity due to their Cu-free compositions and low resistance to IGC due to their coarse grain structures.

4. Summary

In order to examine intrinsic hydrogen embrittlement behavior of 6XXX-series aluminum alloys during fatigue fracture, the ternary Al-Mg-Si alloy was subjected to the fatigue test under controlled experimental humidity with the comparison AA6061 alloy of the same Mg and Si compositions. Additionally, the effect of additive elements such as Cu, Cr and Fe to the ternary alloy on a hydrogen embrittlement (HE) behavior was examined. The following results were obtained.

1. Although the effect of experimental humidity on the 6061 alloy was not so significant, the cyclic lives of the Al-Mg-Si alloy clearly decreased with experimental humidity. This suggested that the Al-Mg-Si alloy exhibited HE by hydrogen atoms intruded from experimental environment.
2. The fracture surface of the Al-Mg-Si alloy showed brittle intergranular cracking (IGC) near its fatigue crack initiation site, and the area of the IGC region increased with the experimental humidity. From these results, the decrease in cyclic lives of the Al-Mg-Si alloy with the experimental humidity was probably attributed to accelerated fatigue crack growth at its early growth stage by the occurrence of IGC near the crack initiation site.
3. Only Cu exhibited the effect of decreasing the HE sensitivity of the Al-Mg-Si alloy in the fatigue fracture among the additive elements examined, Cu, Cr and Fe. The addition of Cu inhibited the occurrence of IGC near the crack initiation site and showed as long cyclic lives under RH90% as under DNG.

References

[1] G. A. Young Jr., J. R. Scully: Metal. and Mater. Trans. A, 33A (2002), 101-115.

[2] S. Osaki, H. Kondo and K. Kinoshita: Mater. Trans., 47(2006), 1127-1134.